Available online at www.sciencedirect.com
SCIENCE DIRECT®
Physics Letters B 578 (2004) 276–284
PHYSICS LETTERS B
www.elsevier.com/locate/physletb

First observation of the $K_S \to \pi^0\gamma\gamma$ decay

NA48 Collaboration

A. Lai, D. Marras

Dipartimento di Fisica dell'Università e Sezione dell'INFN di Cagliari, I-09100 Cagliari, Italy

J.R. Batley, R.S. Dosanjh, T.J. Gershon, G.E. Kalmus, C. Lazzeroni, D.J. Munday, E. Olaiya, M.A. Parker, T.O. White, S.A. Wotton

Cavendish Laboratory, University of Cambridge, Cambridge, CB3 0HE, UK [1]

R. Arcidiacono [2], G. Barr [3], G. Bocquet, A. Ceccucci, T. Cuhadar-Dönszelmann, D. Cundy [4], N. Doble [5], V. Falaleev, L. Gatignon, A. Gonidec, B. Gorini, P. Grafström, W. Kubischta, A. Lacourt, A. Norton, B. Panzer-Steindel, G. Tatishvili [6], H. Wahl [7]

CERN, CH-1211 Genève 23, Switzerland

C. Cheshkov, P. Hristov, V. Kekelidze, D. Madigojine, N. Molokanova, Yu. Potrebenikov, A. Zinchenko

Joint Institute for Nuclear Research, Dubna, Russian Federation

V. Martin, P. Rubin [8], R. Sacco, A. Walker

Department of Physics and Astronomy, University of Edinburgh, JCMB King's Buildings, Mayfield Road, Edinburgh, EH9 3JZ, UK

M. Contalbrigo, P. Dalpiaz, J. Duclos, P.L. Frabetti, A. Gianoli, M. Martini, F. Petrucci, M. Savrié

Dipartimento di Fisica dell'Università e Sezione dell'INFN di Ferrara, I-44100 Ferrara, Italy

A. Bizzeti [9], M. Calvetti, G. Collazuol, G. Graziani, E. Iacopini, M. Lenti, F. Martelli [10], M. Veltri [10]

Dipartimento di Fisica dell'Università e Sezione dell'INFN di Firenze, I-50125 Firenze, Italy

0370-2693/$ – see front matter
doi:10.1016/j.physletb.2003.10.073

M. Eppard, A. Hirstius, K. Holtz, K. Kleinknecht, U. Koch, L. Köpke, P. Lopes da Silva, P. Marouelli, I. Mestvirishvili, I. Pellmann, A. Peters, S.A. Schmidt, V. Schönharting, Y. Schué, R. Wanke, A. Winhart, M. Wittgen

Institut für Physik, Universität Mainz, D-55099 Mainz, Germany [11]

J.C. Chollet, L. Fayard, L. Iconomidou-Fayard, G. Unal, I. Wingerter-Seez

Laboratoire de l'Accélérateur Linéaire, IN2P3-CNRS, Université de Paris-Sud, 91898 Orsay, France [12]

G. Anzivino, P. Cenci, E. Imbergamo, P. Lubrano, A. Mestvirishvili, A. Nappi, M. Pepe, M. Piccini

Dipartimento di Fisica dell'Università e Sezione dell'INFN di Perugia, I-06100 Perugia, Italy

R. Casali, C. Cerri, M. Cirilli [13], F. Costantini, R. Fantechi, L. Fiorini, S. Giudici, I. Mannelli, G. Pierazzini, M. Sozzi

Dipartimento di Fisica, Scuola Normale Superiore e Sezione dell'INFN di Pisa, I-56100 Pisa, Italy

J.B. Cheze, M. De Beer, P. Debu, F. Derue, A. Formica, R. Granier de Cassagnac, G. Gouge, G. Marel, E. Mazzucato, B. Peyaud, R. Turlay, B. Vallage

DSM/DAPNIA, CEA Saclay, F-91191 Gif-sur-Yvette, France

M. Holder, A. Maier, M. Ziolkowski

Fachbereich Physik, Universität Siegen, D-57068 Siegen, Germany [14]

C. Biino, N. Cartiglia, F. Marchetto, E. Menichetti, N. Pastrone

Dipartimento di Fisica Sperimentale dell'Università e Sezione dell'INFN di Torino, I-10125 Torino, Italy

J. Nassalski, E. Rondio, M. Szleper, W. Wislicki, S. Wronka

Soltan Institute for Nuclear Studies, Laboratory for High Energy Physics, PL-00-681 Warsaw, Poland [15]

H. Dibon, M. Jeitler, M. Markytan, I. Mikulec, G. Neuhofer, M. Pernicka, A. Taurok, L. Widhalm

Österreichische Akademie der Wissenschaften, Institut für Hochenergiephysik, A-1050 Wien, Austria [16]

Received 19 September 2003; accepted 20 October 2003

Editor: W.-D. Schlatter

Abstract

Using the NA48 detector at the CERN SPS, 31 $K_S \to \pi^0\gamma\gamma$ candidates with an estimated background of 13.7 ± 3.2 events have been observed. This first observation leads to a branching ratio of $\mathrm{BR}(K_S \to \pi^0\gamma\gamma)_{z>0.2} = (4.9 \pm 1.6_{\mathrm{stat}} \pm 0.9_{\mathrm{syst}}) \times 10^{-8}$ in agreement with Chiral Perturbation Theory predictions.

1. Introduction

Radiative non-leptonic rare kaon decays have proven to be useful tests for low energy hadron dynamics studied in the framework of the Standard Model by the Chiral Perturbation Theory (χPT). This Letter describes the first observation of the $K_S \to \pi^0\gamma\gamma$ decay obtained from data taken by the NA48 experiment in the year 2000.

In the decay $K_S \to \pi^0\gamma\gamma$, the photon pair production is theoretically described by an amplitude dominated by a pseudo-scalar meson pole. In χPT this pole is dominated by the π^0 contribution, and the tree level amplitude is non-vanishing, in contrast to the similar $K_L \to \gamma\gamma$ decay. The leading order theoretical prediction for the branching ratio is 3.8×10^{-8} with higher order corrections expected to be small [1] and is quoted in the kinematic region $z = m^2_{\gamma\gamma}/m^2_K > 0.2$ which is free from the overwhelming $K_S \to \pi^0\pi^0$ background. A measurement of the branching ratio can provide information about the presence of extra non-pole contributions studied, e.g., in [2]. In addition, the momentum dependence of the weak vertex which is predicted by χPT can be tested by the measured shape of the z spectrum. The lowest previously published limit on the branching ratio is $\mathrm{BR}(K_S \to \pi^0\gamma\gamma)_{z>0.2} < 3.3 \times 10^{-7}$ at 90% confidence level [3].

2. Experimental set-up and data taking

The NA48 detector was designed to measure direct CP violation in the decays of K_L and K_S into $\pi\pi$, described by the parameter $\mathrm{Re}(\varepsilon'/\varepsilon)$, using simultaneous far- and near-target beams [4]. The analysis presented in this Letter is based on data recorded during a special 40-day run performed in the year 2000 with near-target beam only and with an intensity of about $\sim 10^{10}$ 400 GeV protons hitting the target during the 3.2 s long SPS spill. The exit of the collimator, 6 m downstream of the target, is followed by a wide vacuum tube approximately 113 m long containing the de-

[1] Funded by the UK Particle Physics and Astronomy Research Council.

[2] On leave from Dipartimento di Fisica Sperimentale dell'Università e Sezione dell'INFN di Torino, I-10125 Torino, Italy.

[3] Present address: University of Oxford, Keble Road, Oxford, OX1 3RH, UK.

[4] Present address: Istituto di Cosmogeofisica del CNR di Torino, I-10133 Torino, Italy.

[5] Also at Dipartimento di Fisica dell'Università e Sezione dell'INFN di Pisa, I-56100 Pisa, Italy.

[6] On leave from Joint Institute for Nuclear Research, Dubna 141980, Russian Federation.

[7] Also at Dipartimento di Fisica dell'Università e Sezione dell'INFN di Ferrara, I-441000 Ferrara, Italy.

[8] On leave from the University of Richmond, Richmond, VA, 23173, USA; Funded in part by the US National Science Foundation under grant 9971970.

[9] Dipartimento di Fisica dell'Universita di Modena e Reggio Emilia, via G. Campi 213/A, I-41100 Modena, Italy.

[10] Istituto di Fisica, Università di Urbino, I-61029 Urbino, Italy.

[11] Funded by the German Federal Minister for Research and Technology (BMBF) under contract 7MZ18P(4)-TP2.

[12] Funded by Institut National de Physique des Particules et de Physique Nucléaire (IN2P3), France.

[13] Present address: Dipartimento di Fisica dell'Università di Roma "La Sapienza" e Sezione dell'INFN di Roma, 00185 Roma, Italy.

[14] Funded by the German Federal Minister for Research and Technology (BMBF) under contract 056SI74.

[15] Supported by the Committee for Scientific Research grants 5P03B10120, SPUB M/CERN/P03/DZ210/2000 and SPB/CERN/P03/DZ146/2002.

[16] Funded by the Austrian Ministry for Traffic and Research under the contract GZ 616.360/2-IV GZ 616.363/2-VIII, and by the Fonds für Wissenschaft und Forschung FWF Nr. P08929-PHY.

cay region and terminated by an aluminium window close to the detector.[17]

The detector elements used in the analysis are the following:

- A liquid krypton calorimeter (LKr) [5], placed less than 2 m behind the aluminium window, is used to measure the energy, position and time of electro-magnetic showers. The energy resolution is

$$\frac{\sigma(E)}{E} \simeq \frac{0.090}{E} \oplus \frac{0.032}{\sqrt{E}} \oplus 0.0042, \quad (1)$$

  where E is in GeV. The position and time resolutions for a single photon with energy larger than 20 GeV are better than 1.3 mm and 300 ps, respectively.
- A sampling hadron calorimeter composed of 48 steel plates, interleaved with scintillator planes, with a readout in horizontal and vertical projections.
- Seven ring shaped scintillator counters equipped with iron converters (AKL), used to detect photons escaping the outer limits of the calorimeter acceptance.

The trigger decision, common to $\pi^0\gamma\gamma$ and $\pi^0\pi^0$ decays, is based on quantities which are derived from the projections of the energy deposited in the electromagnetic liquid krypton calorimeter [6]. The trigger required that the total deposited energy E_{tot} is larger than 50 GeV, the radial distance of the energy deposition centre of gravity from the beam axis is smaller than 15 cm and the proper life time of the kaon is less than 9 K_S lifetimes downstream of the collimator. The inefficiency of the trigger was measured to be $\lesssim 0.1\%$.

More about the detector and the experimental configuration during data taking in the year 2000 can be found in [7].

[17] In the usual NA48 experimental configuration the vacuum tube is terminated at 89 m by a thin Kevlar window followed by a helium filed tank which contains drift chambers and a spectrometer magnet. For these data, however, the Kevlar window and the drift chambers were removed, the helium tank was evacuated and the magnet was switched off.

3. Event selection

The energies and positions of electro-magnetic showers measured in the liquid krypton calorimeter, are interpreted as initiated by photons and are used to calculate the kaon energy and decay vertex. To select $K_S \to \pi^0\gamma\gamma$ and $K_S \to \pi^0\pi^0$ candidates, all events with $\geqslant 4$ clusters are considered. All combinations of four clusters which are within 5 ns from the average time and with no other cluster with energy > 1.5 GeV closer in time than 7 ns with respect to the event time are selected. The event time is computed from the times of the most energetic cells of the selected clusters. In addition, the cluster combination must pass the following cuts:

- To guarantee the appropriate reconstruction quality, the energy of each cluster must be greater than 3 GeV and less than 100 GeV.
- The distance between two clusters is required to be greater than 10 cm to avoid shower sharing effects.
- The total energy of the selected cluster combination is required to be less than 170 GeV and greater than 70 GeV.
- The distance of the centre of gravity of the energy deposition from the beam axis,

$$R_C = \frac{\sqrt{\left(\sum_i E_i x_i\right)^2 + \left(\sum_i E_i y_i\right)^2}}{\sum_i E_i}, \quad (2)$$

  is required to be less than 5 cm, where E_i, x_i, y_i are the ith cluster energy, x and y coordinates at LKr, respectively.

On top of these requirements for each selected event the energy deposited in the hadron calorimeter must not exceed 3 GeV in a time window of ± 15 ns around the event time and the AKL counter should not register any hit in a time window of ± 7 ns around the event time.

The decay vertex position z_{vertex} of a kaon is calculated using the kaon mass constraint,

$$z_{\text{vertex}} = z_{\text{LKr}} - \frac{\sqrt{\sum_{i,j>i} E_i E_j d_{ij}^2}}{m_K}, \quad (3)$$

where z_{LKr} is the longitudinal coordinate of the LKr calorimeter with respect to the end of the collimator and d_{ij} is the distance between ith and jth cluster at the calorimeter. The invariant mass of photon pairs is calculated using z_{vertex}.

The $K_S \to \pi^0\gamma\gamma$ candidates must have a photon pair with an invariant mass within 2 MeV/c^2 of the π^0 mass, m_{π^0}, and the other pair must satisfy the condition $m^2_{\gamma\gamma}/m^2_K > 0.2$. In the $K_S \to \pi^0\pi^0$ sample a χ^2 cut of 27 ($\sim 5\sigma$) is applied to the invariant masses of photon pairs, defined as

$$\chi^2 = \left[\frac{(m_1+m_2)/2 - m_{\pi^0}}{\sigma_+}\right]^2 + \left[\frac{(m_1-m_2)/2}{\sigma_-}\right]^2, \tag{4}$$

where $\sigma_\pm$ are the resolutions on $(m_1 \pm m_2)/2$ measured from the data and parametrised as a function of the lowest photon energy. The typical value of σ_+ is 0.4 MeV/c^2 and σ_- is 0.8 MeV/c^2 [8]. For $K_S \to \pi^0\gamma\gamma$ candidates the χ^2 is required to be larger than 5400.

In order to suppress the large background from $K_S \to \pi^0\pi^0_D$ ($\pi^0_D \to e^+e^-\gamma$) decays with one particle escaping the acceptance the decay region was restricted to be between -1 m and 8 m with respect to the exit of the collimator. Most of the $K_S \to \pi^0\pi^0_D$ background events have an apparent z_{vertex} downstream of this region because of the missing energy. This condition is even more effective against background from $K_L \to \pi^0\pi^0\pi^0$. The $K_S \to \pi^0\pi^0_D$ background is further suppressed by imposing the π^0 mass hypothesis on the remaining four pairings[18] of photon showers and calculating the vertex positions z_{π^0} for each of these γ pairs. Denoting as $z^*_{\pi^0}$ the closest z_{π^0} to the exit of the collimator, events with

$$z^*_{\pi^0} < -4.5 \text{ m} \quad \text{or} \quad z^*_{\pi^0} > z_{\text{vertex}} + 10 \text{ m} \tag{5}$$

are accepted (Fig. 1). This cut is very effective in suppressing $K_S \to \pi^0\pi^0_D$ background because, as shown by Monte Carlo studies, this background is completely dominated by events with one of the $\pi^0_D \to ee\gamma$ decay products escaping detection. In addition, this cut removes events from inelastic scattering of beam particles in the collimator with multiple π^0 production. The downstream end of this cut is intentionally extended in

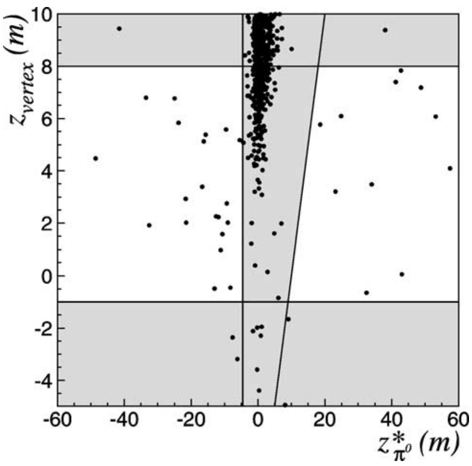

Fig. 1. Illustration of z_{vertex} and $z^*_{\pi^0}$ cuts on the data. All other cuts were applied. Rejected areas are shaded. Both variables are defined with respect to the exit of the collimator. The accumulation of events around small $z^*_{\pi^0}$ values is due to $K_S \to \pi^0\pi^0_D$ background at high z_{vertex} and due mainly to pile-up events at low or negative z_{vertex}.

order to reduce background from pile-up of a π^0 from $K_S \to \pi^0\pi^0$ with γ's from another decay.

A small amount of $K_S \to \pi^0\pi^0_D$ background survives the above cuts if a γ from one π^0 and a γ or an e from the other π^0 overlap. In this case the reconstructed z_{vertex} does not move downstream because the entire kaon energy is collected in the LKr calorimeter and there is no pair of showers which would give a correct z_{π^0} under a π^0 hypothesis. Still, by assuming this type of overlap the correct vertex position can be reconstructed by

$$z_{\text{overlap}} = z_{\text{LKr}} - \frac{1}{m_{\pi^0}}\sqrt{E_1 d^2_{14}\frac{\sum_{j>1,i>j}^4 E_i E_j d^2_{ij}}{\sum_i^3 E_i d^2_{i4}}}, \tag{6}$$

where index 1 refers to the γ from the π^0, indexes 2 and 3 to γ or e's from π^0_D and index 4 to the overlapping shower. For $\pi^0\gamma\gamma$ events $z_{\text{overlap}} \neq z_{\text{vertex}}$ and hence a cut $|z_{\text{overlap}} - z_{\text{vertex}}| > 1.5$ m on all 12 possible combinations reduces this type of background to a sufficiently low level, without significant loss of signal.

In order to remove events with hadrons or overlapping showers from the $\pi^0\gamma\gamma$ sample, the shower width is required to be less than 3σ above the average value for photon showers of a given energy. This

[18] If indexes 1 and 2 refer to γ's assigned to the π^0 then these four pairings are 1–3, 1–4, 2–3 and 2–4.

cut, which is calibrated using showers in $K_S \to \pi^0\pi^0$ decays, removes $< 1\%$ of good $K_S \to \pi^0\gamma\gamma$ events.

In addition, residual background from $\Xi^0 \to \Lambda\pi^0$ with subsequent $\Lambda \to n\pi^0$ decay, where one γ escapes and the neutron produces a photon-like shower in the LKr calorimeter, is suppressed by exploiting the large momentum asymmetries in both Ξ^0 and Λ decays and accepting only events with:

$$\frac{|E_3 - E_4|}{E_3 + E_4} < 0.35,$$
$$\frac{(E_3 + E_4) - (E_1 + E_2)}{E_1 + E_2 + E_3 + E_4} < 0.3, \tag{7}$$

where indexes 1 and 2 refer to the shower pair identified as photons from the π^0 and 3, 4 to other two showers.

The background from accidental pile-up events is reduced by strengthening the requirements on shower times. Two configurations of a pile-up are considered: $3 + 1$ showers and $2 + 2$ showers. The $3 + 1$ configuration is best described by a variable

$$t_{3\,\max} = \left[t_i - \sum_{j \neq i} t_j/3 \right]_{\max}, \tag{8}$$

where the difference between any shower time and the average of the other three is maximised. Similarly, for the $2 + 2$ configuration one can use a variable

$$t_{2\,\max} = \left[t_i - \sum_{j \neq i} t_j/2 \right]_{\max} \tag{9}$$

in which only two of three remaining shower times are averaged. For the $3 + 1$ pile-up topology $t_{2\,\max}$ and $t_{3\,\max}$ are always equal within the time resolution, however in the $2+2$ case the two variables have different values in principle. This allows one to analyse this type of background in more detail. For the selection of the signal sample a single cut on $t_{2\,\max}$ of < 1 ns is chosen, because $t_{2\,\max}$ describes both configurations in the same way.

After all selection cuts 31 events remain in the sample. For the normalisation a sample scaled-down by factor 1000 of about 285×10^3 $K_S \to \pi^0\pi^0$ events has been used.

4. Background subtraction

The following processes have been considered as potential sources of residual background:

- Irreducible $K_L \to \pi^0\gamma\gamma$ background from the K_L component of the beam;
- $K_S \to \pi^0\pi^0$ with mis-reconstructed energy;
- $K_S \to \pi^0\pi^0_D$ with a γ or an e escaping detection or with a shower overlap;
- Hadron background, mainly $\Xi^0 \to \Lambda\pi^0$ with subsequent $\Lambda \to n\pi^0$, with three photon showers and one narrow neutron shower in the LKr calorimeter;
- Pile-up of two decays where the two decaying particles originate at the target either from two protons (accidental pile-up) or from a single proton (in-time pile-up).

The amount of $K_L \to \pi^0\gamma\gamma$ admixture in the signal sample is estimated using the K_L flux measured from the $K_S \to \pi^0\pi^0$ rate assuming equal production of K_S and K_L at the target. The acceptance was calculated using the same Monte Carlo simulation as used for the $K_S \to \pi^0\gamma\gamma$ acceptance calculation described in Section 5. This background amounts to 3.8 ± 0.2 events.

$K_S \to \pi^0\pi^0$ events can pass the cuts on invariant masses, and especially $\chi^2 > 5400$, only if far non-Gaussian tails are present in the energy reconstruction from the LKr calorimeter. In order to study cases where one of the four shower energies may be mis-reconstructed, making use of the over-constrained kinematics of $K_S \to \pi^0\pi^0$ events, the invariant mass of the event is reconstructed by using only three out of four shower energies and all four positions. None of the signal events has been found to have an invariant mass close to the kaon mass in any of the shower combinations. In addition, a toy Monte Carlo was employed to generate $K_S \to \pi^0\pi^0$ events using realistic resolutions and non-Gaussian tails in energy. To probe an extreme case the probability of non-Gaussian tails was enhanced by an order of magnitude with respect to that known from E/p studies of electrons from the $\mathrm{Re}(\varepsilon'/\varepsilon)$ analysis [8]. In a sample equivalent to twice the flux of the 2000 near-target run no event passes the χ^2, $m_{\gamma\gamma}$ and z_{vertex} cuts at the same time.

The residual $K_S \to \pi^0\pi^0_D$ background has been studied using full Monte Carlo simulations. Generating 1.7 times the collected flux, 4 events have been found to pass all cuts. Three of them have overlapping showers and reside in the tail of the $z_{\text{overlap}} - z_{\text{vertex}}$ distribution. The fourth event decays in the collimator, and one of the photons undergoes a conversion in the collimator walls, while the e^+e^- pair from the π^0 passes trough the central hole of the detector. Scaling these events to the observed kaon flux, a background estimate of 2.4 ± 1.2 events is obtained with an uncertainty dominated by the statistics. The systematic error of this estimate has been checked by relaxing $z^*_{\pi^0}$ and z_{overlap} cuts. The number of events and their z_{vertex} distribution agree with data within few percent.

The amount of hadron background surviving cuts on the energy deposited in the hadron calorimeter, the shower width and the energy asymmetry (7) was estimated by extrapolating the shower width distribution from large widths to the signal region. The shower width distribution of neutrons was extracted from fully reconstructed $\Xi^0 \to \Lambda\pi^0 \to n\pi^0\pi^0$ events. An estimate of 0.1 ± 0.1 events has been obtained, with an uncertainty determined by the limited knowledge of the extrapolation shape.

The accidental pile-up background has been studied using time variables $t_{2\,\max}$ (9) and $t_{3\,\max}$ (8) in a time window of 6 ns which is six times larger than the signal time window. In this time window the event distribution is not affected by any selection cut. It turns out that about 50% of the background is in a $3+1$ configuration while 50% is $2+2$. Since both of these configurations are described equivalently by $t_{2\,\max}$ this variable is used to extrapolate from the control region $2 < |t_{2\,\max}| < 6$ ns to the signal region $|t_{2\,\max}| < 1$ ns assuming a fat distribution. This extrapolation gives an estimate of 7.0 ± 1.3 events for the accidental pile-up background. The order of magnitude of this estimate was confirmed by overlaying 3-photon events from a $K_S \to \pi^0\pi^0$ toy Monte Carlo with random showers detected close in time (20–30 ns) to fully reconstructed $K_S \to \pi^0\pi^0$ events and by taking into account the kaon flux.

The in-time pile-up background in general has a topology similar to the accidental pile-up, but, since it is generated by the same proton in the target, its rate cannot be measured by extrapolating from the out-of-time sample. The relative rate of in-time and accidental pile-up has been studied using fully reconstructed $K_S \to \pi^0\pi^0$ with additional showers in the LKr calorimeter. It has been found that a 20% enhancement of pile-up background due to an in-time component cannot be excluded. In order to estimate the amount of total pile-up background without using time variables, the distribution of R_C has been employed. The background is extrapolated from a control region $7 < R_C < 10$ cm to the signal region $R_C < 5$ cm by using the R_C shape obtained from the out-of-time sample in the $t_{2\,\max}$ control region. This extrapolation leads to an estimate of 6.8 ± 2.9 events for both in-time and accidental pile-up backgrounds. The uncertainty takes into account the statistical error of the data in the control region as well as the uncertainty of the extrapolation which is determined by the statistics of the out-of-time sample. This measurement is in good agreement with previous considerations and, since it contains the least number of assumptions, it is used for the branching ratio calculation. As can be seen from Fig. 2, the $K_S \to \pi^0\pi^0_D$ background is not double-counted in this subtraction because it populates the $R_C < 7$ cm region.

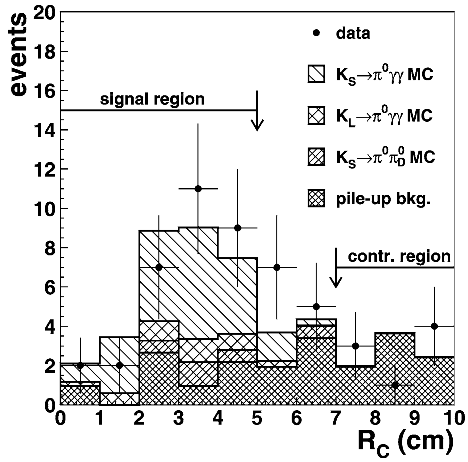

Fig. 2. The R_C distribution of data compared to the sum of background models and signal Monte Carlo scaled by the calculated branching ratio. The control region for pile-up background subtraction is indicated.

Recently, the $K_S \to \pi^0e^+e^-$ decay has been observed for the first time. Using the measured branching ratio [9] and taking into account the cutoff on the invariant mass of the e^+e^- pair $m^2_{ee}/m^2_K > 0.2$ this background has been estimated to contribute 0.6 ± 0.3 events.

5. Result

Of the selected 31 events, 13.7 ± 3.2 are estimated to be background (Table 1). The probability to observe 31 or more events in absence of a signal with a background of 13.7 ± 3.2 events is 1.5×10^{-3}. Subtraction of the background from the selected sample leads to a signal of 17.3 ± 6.4 events. In the control region, defined as $3 < |m_{12} - m_{\pi^0}| < 5\ \text{MeV}/c^2$, the observed data agree well with the background estimate (Fig. 3).

The detector acceptances of the $K_S \to \pi^0\gamma\gamma$ decay and of the normalisation decay channel $K_S \to \pi^0\pi^0$ were calculated using a full Monte Carlo simulation of the detector based on GEANT [10].[19] The $K_S \to \pi^0\pi^0$ acceptance was determined to be $(18.6 \pm 0.1)\%$. The $K_S \to \pi^0\gamma\gamma$ generator used the decay matrix element calculated by [1] using χPT. The acceptance of the $K_S \to \pi^0\gamma\gamma$ for $z > 0.2$ is $(7.2 \pm 0.3)\%$, where the dominant contribution to the uncertainty is extracted from the comparison with a simulation using a pure phase-space decay generator. The $K_S \to \pi^0\gamma\gamma$ acceptance is smaller than that of $K_S \to \pi^0\pi^0$ mainly due to cuts on $z^*_{\pi^0}$ and energy asymmetry defined in (5) and (7).

Normalising the signal to the collected $K_S \to \pi^0\pi^0$ sample and taking into account the acceptances results in a ratio of decay widths

$$\frac{\Gamma(K_S \to \pi^0\gamma\gamma)_{z>0.2}}{\Gamma(K_S \to \pi^0\pi^0)} = (1.57 \pm 0.51_{\text{stat}} \pm 0.29_{\text{syst}}) \times 10^{-7}, \quad (10)$$

Table 1
Summary of background composition in both signal and control regions, the latter being defined as $3 < |m_{12} - m_{\pi^0}| < 5\ \text{MeV}/c^2$, compared to data

Events in	Signal region	Control region
$K_L \to \pi^0\gamma\gamma$ background	3.8 ± 0.2	0.1 ± 0.0
$K_S \to \pi^0\pi^0_D$ background	2.4 ± 1.2	4.2 ± 1.6
Hadronic background	0.1 ± 0.1	0.1 ± 0.1
Pile-up background	6.8 ± 2.9	4.3 ± 2.0
$K_S \to \pi^0 e^+ e^-$ background	0.6 ± 0.3	$\ll 0.1$
Total background	13.7 ± 3.2	8.7 ± 2.6
Data	31	9

[19] In order to speed up the simulation, electromagnetic showers are pre-generated and stored in a shower library.

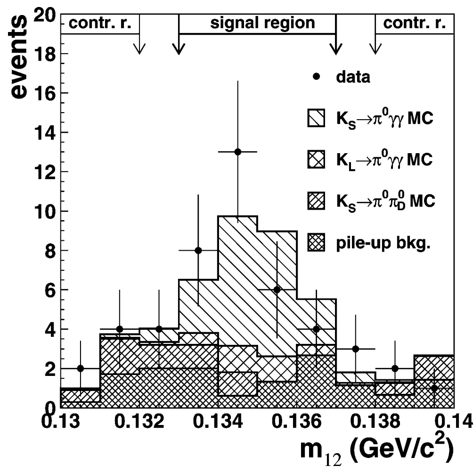

Fig. 3. The invariant mass distribution of the photon pair assigned to the π^0. The data in the control region are compatible with background while the signal region contains a conspicuous excess indicating a $K_S \to \pi^0\gamma\gamma$ signal.

where the systematic uncertainty takes into account the background subtraction and acceptance calculation uncertainties. This result is stable against variations of most relevant cuts. In particular, the result does not change significantly by releasing the cut on the AKL anti-counter which increases the pile-up background by a factor 5, and when requiring no associated hit in a scintillator hodoscope placed upstream of the LKr calorimeter, which reduces the $K_S \to \pi^0\pi^0_D$ background by a factor 3. Uncertainties on energy scale and linearity of the energy measurement are negligible. Using $\text{BR}(K_S \to \pi^0\pi^0)$ from [11], one obtains

$$\text{BR}(K_S \to \pi^0\gamma\gamma)_{z>0.2} = (4.9 \pm 1.6_{\text{stat}} \pm 0.9_{\text{syst}}) \times 10^{-8} = (4.9 \pm 1.8) \times 10^{-8} \quad (11)$$

which agrees with the predictions of [1].

In order to test the momentum dependence of the weak vertex predicted by the χPT the z distribution of the sample after background subtraction has been compared to z distributions of simulated $K_S \to \pi^0\gamma\gamma$ events using two decay generators, one with the χPT matrix element and one with pure phase space. Fig. 4 shows that both calculations agree within errors with the data and more statistics would be needed to prove the chiral structure of the weak vertex.

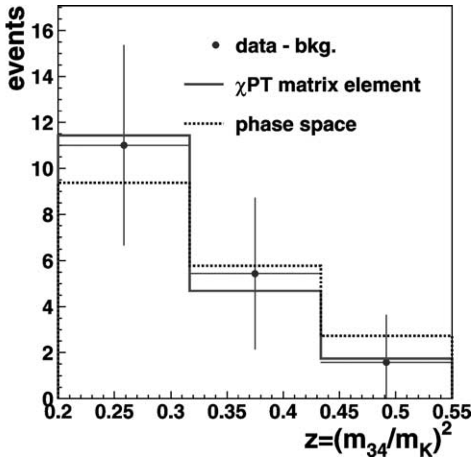

Fig. 4. The z distribution of data after background subtraction compared to a Monte Carlo $K_S \to \pi^0\gamma\gamma$ simulation using phase space (dashed line) and χPT matrix element [1] (continuous line) in the decay generator.

6. Conclusions

A first observation of the decay $K_S \to \pi^0\gamma\gamma$ has been made. The branching ratio has been calculated in the kinematic region $z = m^2_{\gamma\gamma}/m^2_K > 0.2$, which is the one considered in the theoretical prediction [1] based on χPT. The measured value $\mathrm{BR}(K_S \to \pi^0\gamma\gamma)_{z>0.2} = (4.9 \pm 1.6_{\mathrm{stat}} \pm 0.9_{\mathrm{syst}}) \times 10^{-8}$ agrees with the predicted 3.8×10^{-8}. The measured z-spectrum agrees within uncertainties with both phase-space and χPT distributions and more statistics would be needed to prove the chiral structure of the weak vertex.

Acknowledgements

It is a pleasure to thank the technical staff of the participating laboratories, universities and affiliated computing centres for their efforts in the construction of the NA48 apparatus, in the operation of the experiment, and in the processing of data. We would also like to thank G. D'Ambrosio for useful discussions.

References

[1] G. Ecker, A. Pich, E. de Rafael, Phys. Lett. B 189 (1987) 363.
[2] J. Bijnens, E. Pallante, J. Prades, Nucl. Phys. B 521 (1998) 305.
[3] A. Lai, et al., Phys. Lett. B 556 (2003) 105.
[4] N. Doble, et al., Nucl. Instrum. Methods B 119 (1996) 181.
[5] G. Unal, for NA48 Collaboration, in: 9th International Conference on Calorimetry, October 2000, Annecy, France, hep-ex/0012011.
[6] G. Barr, et al., Nucl. Instrum. Methods A 485 (2002) 676.
[7] A. Lai, et al., Phys. Lett. B 551 (2003) 7.
[8] A. Lai, et al., Eur. Phys. J. C 22 (2001) 231.
[9] J.R. Batley, et al., Phys. Lett. B 574 (2003) 43.
[10] GEANT Description and Simulation Tool, CERN Program Library Long Write-up W5013 (1994).
[11] Particle Data Group, http://pdg.web.cern.ch/pdg/ as of May 2003.